Nanoscale Res Lett (2009) 4:1209–1217
DOI 10.1007/s11671-009-9380-0

NANO EXPRESS

Wettability Modification of Nanomaterials by Low-Energy Electron Flux

I. Torchinsky · G. Rosenman

Received: 9 March 2009 / Accepted: 15 June 2009 / Published online: 2 July 2009

Abstract Controllable modification of surface free energy and related properties (wettability, hygroscopicity, agglomeration, etc.) of powders allows both understanding of fine physical mechanism acting on nanoparticle surfaces and improvement of their key characteristics in a number of nanotechnology applications. In this work, we report on the method we developed for electron-induced surface energy and modification of basic, related properties of powders of quite different physical origins such as diamond and ZnO. The applied technique has afforded gradual tuning of the surface free energy, resulting in a wide range of wettability modulation. In ZnO nanomaterial, the wettability has been strongly modified, while for the diamond particles identical electron treatment leads to a weak variation of the same property. Detailed investigation into electron-modified wettability properties has been performed by the use of capillary rise method using a few probing liquids. Basic thermodynamic approaches have been applied to calculations of components of solid–liquid interaction energy. We show that defect-free, low-energy electron treatment technique strongly varies elementary interface interactions and may be used for the development of new technology in the field of nanomaterials.

Keywords Nanomaterials · Wettability · Low-energy electron irradiation · Thermodynamic properties

I. Torchinsky · G. Rosenman (✉)
Department of Physical Electronics, School of Electrical Engineering, Tel Aviv University, Tel Aviv 69978, Israel
e-mail: gilr@eng.tau.ac.il

I. Torchinsky
e-mail: ilya@eng.tau.ac.il

Introduction

Finely divided submicron and nanoscale solid materials demonstrate anomalous properties at both nano- and microscales due to their huge surface energy and high specific surface area. They are considered today as building blocks in many nanotechnological applications related to electronics, optics and biomedicine [1]. Many diverse fundamental surface-related physical properties of nanomaterials such as wettability, dispersion, hygroscopicity and agglomeration define key nanotechnological processes [2].

The common physical property of nanomaterials is to create macroscopic aggregates. For example, cohesion followed by agglomeration easily occurs among ZnO nanoparticles due to their huge specific surface area, high intrinsic surface energy [3] as well as pyroelectric electrostatic interaction [4]. Agglomeration leads to a nonuniform density distribution of the nanomaterials. However, the most obvious effect of agglomeration is losing of individual physical properties of nanoparticles, especially physical properties provided by quantum-size effects. Self-assembled nanomaterials strongly demonstrate different basic features and figures of merit compared to individual nanoparticles of the same composition. Thus, nanopowder surface modification, preventing or strengthening cohesion and agglomeration of nanoparticles, is a critical issue in nanotechnology [5].

Fundamental studies [6, 7] have been recently undertaken to understand interparticle forces leading to assembly or nonassembly of nanoparticles. Numerous research works on fine nanomaterial surface treatment technology have been directed to change their affinity to agglomeration. It has been shown that aggregation can be prevented by protecting nanoparticles using polymer or surfactant monolayers. Another way is electrical charging electrostatic

stabilization, which is used in aqueous solutions where the particles are surrounded by a hydration layer, preventing their coalescence [7]. Various "encapsulation" technologies have been applied using different chemical materials, to decrease or to increase the nanoparticles surface energy and their intrinsic affinity to cohesion and agglomeration [8–10]. It has become clear that wettability is a critical factor in the creation of nanoparticle clusters [7]. The surface modification of nanomaterials, providing transition from hydrophobic (low surface energy) to hydrophilic (high surface energy) state or vice versa, has many potential applications in many fields of modern nanotechnology such as prevention of aggregation of the particles [11], modification of chemical stability, variation of their tribological properties and improving biocompatibility of nanomaterials [12].

Recently, a new approach has been developed by us to modify materials surface free energy and many related properties [13] such as wettability [14], bonding [15], etching [16] and biocompatibility [17, 18]. This technique is based on combination of ultraviolet (UV) illumination and low-energy electron irradiation. UV treatment is a well-known technique for the surface modification leading to hydrophilicity enhancement of materials [19]. The method of low-energy electron irradiation has been developed in our laboratory for surface energy modification of solid-state materials of different origins [13, 20]. The key principle of the method developed is that the chosen electron energy is much less than the energy threshold of defects creation in irradiated materials. The electron current, incident electron charge and electron energy are coadapted to the electronic structures of the materials when the injected primary electrons and generated secondary electron/hole charges are trapped near the surface at the depth of a few nanometers [21]. We observed this phenomenon in many solid-state materials, such as amorphous SiO_2, S_3N_4, glass, mica, Al_2O_3, n- and p-Si, metal oxides (TiO_2, Al_2O_3, ZnO thin films), biomimetic and biomaterials (sea shells, hydroxyapatite and related calcium phosphates). The wettability of ferroelectric $LiTaO_3$ crystal has been varied in a range of contact angles from high hydrophilic (water contact angle $\theta = 6°$) to hydrophobic state with $\theta = 90°$. It has afforded to find optimal conditions for direct bonding of ferroelectric crystals [15]. Two different mechanisms of hydrophobicity enhancement versus incident electron charge have been found, where one is surface electrostatic charging observed for low level of electron incident charge and the other is formation of ultrathin organic film, which was observed for high-electron doses [21].

In this paper, we apply the method of low-energy electron treatment [13] to powders of different origins, such as diamond and ZnO. Diamond powder possesses exceptional chemical inertness that arises from high atomic density and strong intrinsic covalent bonding [22].The agglomeration of diamond powder is observed for nanoparticles with dimensions less than 100 nm. However, the larger the size of nanoparticles the less is the affinity to agglomeration [23]. Another nanomaterial, ZnO, is unique and widely studied. Its low chemical stability and well-defined catalytic and pyroelectric properties allow observing high affinity to cohesion and agglomeration leading to the formation of various self-assembled nanostructures such as nanowires and nanorings [24]. Photosensitivity of ZnO is the physical reason for photoinduced wettability conversion [25].

The controllable nanoscale modification of surface free energy and related properties described in this work using low-energy electron flux is a new promising concept for nanomaterials and provides a highly potential approach for the development of new nanotechnology. This nanoscale tool has never been used for modification of nanomaterials.

Experimental Setup and Methods

Low-Energy Electron Treatment Technique

In this work, the combination of two different techniques was used for surface energy modification: UV and low-energy electron irradiation. The UV illumination of nanomaterial samples was carried out using nonfiltered, unfocused UV light (185–2,000 nm) generated by a Hg–Xe lamp. The illumination duration was around 5 min, and it always led to hydrophilic state [19]. The electron irradiation was performed using an electron gun (EPG-7, Kimball Physics Inc., USA) in vacuum 10^{-7} Torr at room temperature, using invariable energy of the incident electrons $E_p = 300$ eV. The electron irradiation dose was 360 $\mu C/cm^2$, which provided a high level of electron-induced hydrophobicity. The particles were being shaken during the UV or low-energy electron irradiation in order to irradiate the whole surface of the treated nanomaterial.

Wettability Measurements

Wettability studies on planar solid surfaces are usually conducted by direct contact angle observation. We applied this method to the observation of a macroscopic variation of the nanomaterial wettability. It was roughly estimated by measuring the static contact angles of sessile drops of deionized water (pH 5.5, resistivity >17 MΩ cm). The plastic adjustable volume pipette (Eppendorf Research® pro, Germany) was used.

Macroscopic wettability of nanomaterials was studied using samples fabricated by covering the nanopowder of

the chemically cleaned glass substrate (1 cm^2). No mechanical pressure was applied. The thickness of the studied nanoparticle layers was around 1 mm. The macroscopic wettability state of the samples and glass substrate was estimated by measuring the static contact angles of sessile water drops placed on a sample surface. The volume of the water drops was kept constant at 2 μL over measurements. The measured wettability contact angle of the glass substrate was 15–20°.

Such a direct approach of the contact angle measurements cannot be used for high accuracy wettability measurements on finely dispersed solid materials such as nanomaterials. The conventional investigation method followed in this case is capillary rise technique [26], which leads to a large spectrum of analytical information and is extensively applied in the pharmaceutical industry for wettability studies of nanopowders [27]. Such information is important in drug manufacturing (adhesion or nonadhesion of the component on mixing surface) [28]. However, the capillary rise method strongly limits wettability contact angle measurements to contact angles <90° [32].

In this work, we applied capillary rise wetting technique to our wettability tests of modified nanopowders. In one method, nanoparticles are packed into a tube, one end of which is subsequently immersed into a liquid of known surface tension. The liquid rises through the capillaries formed between the particles within the tubing. The distance traveled by the liquid as function of time is measured. Washburn equation [29] (Eq. 1), which describes the liquid penetration through a compact vertical bed of particles with constant small pore radius, allows us to calculate the contact angle:

$$h^2 = \frac{r_c \gamma_{LV} \cos\theta}{2\mu} t \quad (1)$$

where μ is the liquid viscosity, h is the height of liquid penetration into the powder in time t, γ_{LV} is surface tension of the liquid in equilibrium with the vapor of the liquid, and r_c is radius of the capillary as the powder is considered as a bundle of parallel capillaries of constant radius.

The experimental procedure included several steps. A definite amount of nanoparticles were manually packed in a glass tube (0.5 cm inner diameter and 10 cm long). Before packing with the powder, the glass tubes are thoroughly cleaned with distilled water and then dried at 110 °C. The tube was always filled to the same height and with the same weight for a uniform and constant package of nanoparticles. This column is then placed in upright position in a beaker containing the appropriate probing liquid, and the liquid rise is followed as a function of time. The height was measured with a graduated scale by charge-coupled device camera. The capillary radius r_c (Eq. 1) was determined using *n*-hexane, which was found to completely wet the studied samples. Once the value of r_c was obtained, it was then possible to calculate the contact angle for a given liquid on the powdered surface using the Washburn equation (Eq. 1).

The standard set of 97–99% purity probing liquids possessing well-studied physical properties used in this work were as follows: *n*-hexane, 1-bromonaphthalene, diiodomethane, formamide, ethylene glycol and water. They differ by their viscosity, surface tension, polar and dispersive components, etc. that allow studying the effect of surface modification of nanomaterials using quantitative analyses of wettability data.

Basic Thermodynamic Approaches

The fundamental basis for understanding fine mechanisms of surface modification of nanomaterials is to carry out a detailed investigation into the surface free energy and its components allowing finding elementary interface interactions. Calculation of surface free energy of solid materials is based on measurements of the wettability contact angles of selected polar and apolar liquids deposited on surfaces [30, 31]. The key methods of calculations of critical surface tension, surface free energy and its components applied in this work are those of Zisman [32], Owens–Wendt [33] and a relatively new method of van Oss-Chaudhury-Good [34].

The concept of the critical surface tension was first introduced by Zisman. It is considered as a "wettability index" [32]. Critical surface tension of a material surface is the minimum value of surface tension needed for a liquid to spread completely (i.e., zero contact angle) on that particular surface material. Any liquid whose surface tension equals or is less than γ_{LV} will make a zero contact angle and, accordingly, will completely spread on the surface. According to the Zisman method, the values of the cosines of the contact angles of different liquids on the same surface should be aligned along a straight line:

$$\cos\theta = a + b\gamma_{LV} \quad (2)$$

where γ_{LV} is the surface tension of the liquid.

Owens and Wendt [33] distinguished between the dispersion forces (London forces) and polar forces based on different intermolecular forces (orientation Keesom interaction, induction Debye interaction, Lewis acid/base electron-donating and electron-accepting interaction, hydrogen bonding, etc.). The value of the surface free energy is the sum of two components:

$$\gamma = \gamma^d + \gamma^p \quad (3)$$

where γ is the solid surface free energy, and the index d refers to dispersion, p to polar interactions. Thus, Owens–

Wendt approach allows estimating surface free energy and its polar and dispersive components.

$$\frac{\gamma_L(\cos\theta+1)}{2\left(\gamma_L^d\right)^{1/2}}=\left(\gamma_L^P\right)^{1/2}\frac{\left(\gamma_L^p\right)^{1/2}}{\left(\gamma_L^d\right)^{1/2}}+\left(\gamma_S^d\right)^{1/2}\rightarrow y=mx+b \quad (4)$$

Calculations of thermodynamic properties of the studied powders were carried out on the basis of implemented measurements of wettability contact angles and by using known physical properties of the probing liquids (Table 1).

Studied Powder Materials

Two different sorts of powders of different origins, having different physical properties, particle size and chemical activity, were selected for the wettability studies. The ZnO nanomaterial (EPM-E from Umicore, Belgium) was of 99.4% purity. The surface area was 1–3 m^2/g. The average particle size was 200 nm. The diamond particles (Sinai Yehuda, Israel) had an average size of 1 micron.

SEM Characterization

Environmental scanning electron microscope Quanta 200F (SEM method) was used to characterize ZnO and diamond powders. The samples were prepared by covering the powder on a glass substrate. No any mechanical pressure was applied during the sample preparation.

Experimental Results

SEM Characterization of Powders

The SEM images (Fig. 1) illustrate the structure of as-prepared ZnO and diamond samples. The ZnO nanoparticles (Fig. 1a) are highly agglomerated. There is no any separated individual nanoparticle in the obtained image. The self-assembled ZnO structure exhibits nanorod (nanowires)-like morphology (Fig. 1a). The length and diameter of these nanorods are quite different and range as follows: lengths 1–5 μm, diameters 200–500 nm. They create a nonregular network containing rods (wires) of different orientation and size. The density of this network is nonhomogenous. High dense agglomerates as well as empty regions of 0.1–1.2 μm dimensions are observed (Fig. 1a).

SEM image of the diamond material (Fig. 1b) demonstrates absolutely different physical state of these particles. Diamond grains are approximately of a similar shape and around 1 μm in size. The image neither shows agglomerates nor any trends of these diamond particles to self-assembling.

Macroscopic Wettability of Modified Powder

The Fig. 2 shows the results of contact angle measurements implemented on untreated (Fig. 2a) and electron beam-treated surfaces of ZnO powder (Fig. 2b, c). The water

Table 1 Surface tension (γ_{lv}) and its dispersive (γ_{lv}^d) and polar (γ_{lv}^p) components (in mJ/m^2) of the used probing liquids [35]

Liquids	Surface tension γ_{lv} (mJ/m^2)	Polar component γ_{lv}^p (mJ/m^2)	Dispersive component γ_{lv}^d (mJ/m^2)	Viscosity η (mPa*s)
n-Hexane	18.5	0	18.5	0.00326
1-Bromonaphtalene	44.6	0.9	43.7	4.8
Ethylene glycol	48.2	19.0	29.2	18.3
Diiodomethane	50.8	0.4	50.4	2.76
Formamide	58.4	27.0	31.3	4.15
Water	72.8	51.0	21.8	1

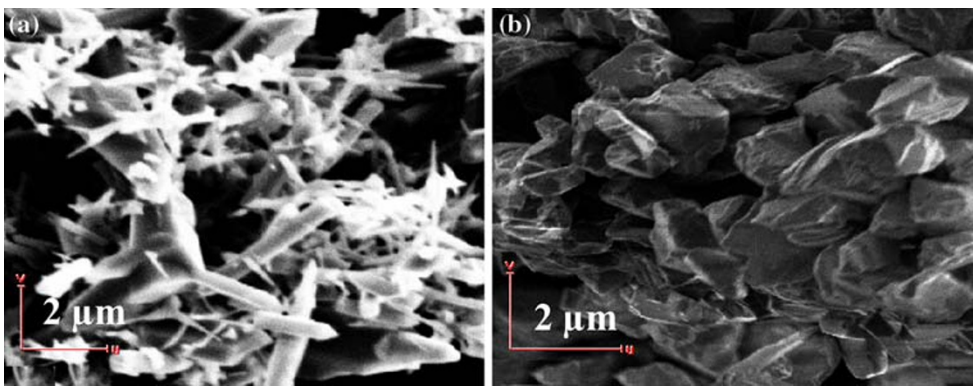

Fig. 1 SEM images of the ZnO (**a**) and diamond (**b**) powders

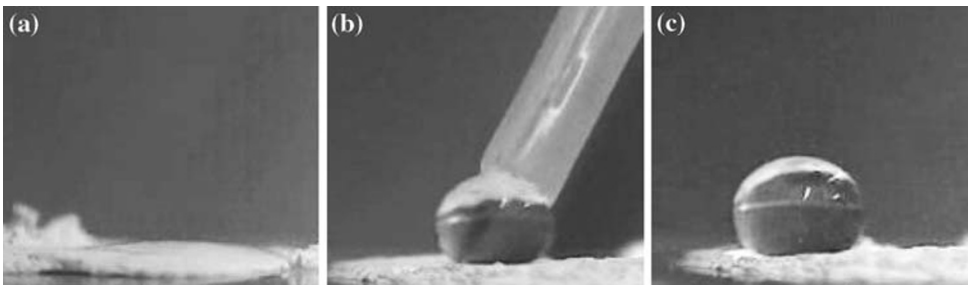

Fig. 2 Optical images collected during macroscopic wettability studies in ZnO nanomaterial sample: **a** water droplet on as-prepared ZnO, **b** and **c** wettability of electron-treated sample surfaces

droplet placed on the sample penetrated inside ZnO nanomaterials very fast in ~1 s showing complete wetting (penetration) (Fig. 2a). The macroscopic contact angle was very small, not more than 3–5°. No difference was found between UV-illuminated and as-prepared ZnO samples.

Electron irradiation dramatically changed the liquid drop behavior on the ZnO nanomaterial sample surface (Fig. 2b, c). The droplet that brought into direct contact with the electron-treated nanopowder surface demonstrated a strong resistance to be placed on the surface. The Fig. 2b shows the deformed droplet shape that was generated by the pipette, pressing the droplet to the surface. We did not succeed in "pasting" the droplet to the surface. Very high hydrophobicity (Fig. 2c) was observed when the droplet was dropped down on the ZnO surface from a height of about 3–5 mm. Sometimes the landing water droplets showed bouncing effect caused by high repelling surface properties, resulting in detachment of the drops.

These results clearly demonstrate that the water droplets completely spread on untreated ZnO nanomaterial surface, while they exhibit opposite, strongly hydrophobic behavior on the electron-treated sample. It should be marked that diamond powder did not reveal any variation of the macroscopic wettability state for all kinds of samples (as-prepared, UV-treated and low-energy electron-irradiated). The water droplet demonstrated a fast penetration between diamond particles.

Wettability Studies (Capillary Rise Technique) and Thermodynamic Properties of Modified Powders

The capillary rise technique [26] allows obtaining exact data on wettability contact angles of powders followed by the application of well-developed thermodynamic approaches for the understanding of interface interactions. The results of the contact angle studies for as-prepared and treated diamond particles using the capillary rise technique are given in Table 2.

These experimental data show that as-prepared diamond powder demonstrates a water contact angle of 75° and possesses moderate hydrophobicity. Both UV and electron beam irradiation change rather feebly the wettability for all studied probing liquids with deviation of the contact angles in a very limited range, i.e. $\Delta\theta \sim 5$–$15°$.

ZnO nanomaterial manifests another behavior showing high affinity to the applied modification methods (Table 3).

The wettability for as-prepared ZnO nanomaterial sample may be defined as slightly hydrophilic with $\theta \sim 60°$. Under UV illumination, water contact angle dropped down to a very small value of about 3°, which is the evidence that UV modification leads ZnO surface to a high hydrophilic state. All tested liquids, except diiodomethane, showed very low contact angle on UV-treated ZnO powder. These data are consistent with the results of the work [36] where high photocatalitic properties of ZnO

Table 2 Contact angle, θ, measured for as-prepared and treated diamond powders, obtained by the capillary rise technique

	1-Bromonaphtalene	Ethylene glycol	Diiodomethane	Formamide	Water
As-prepared diamond powder	35 ± 3	54 ± 2	76 ± 1	62 ± 2	75 ± 1
UV illuminated	38 ± 2	54 ± 2	69 ± 3	52 ± 2	70 ± 1
E-beam irradiated	35 ± 2	70 ± 1	80 ± 2	80 ± 3	84 ± 2

Table 3 Contact angle, θ, measured for as-prepared and treated ZnO nanomaterial

	1-Bromonaphtalene	Ethylene glycol	Diiodomethane	Formamide	Water
As-prepared ZnO nanomaterial	9 ± 1	63 ± 1	66 ± 2	52 ± 3	60 ± 4
UV illuminated	8 ± 2	14 ± 2	64 ± 1	20 ± 3	3 ± 1
E-beam irradiated	8 ± 1	72 ± 1	70 ± 2	73 ± 3	85 ± 2

making it hydrophilic have been found. Low-energy electron treatment strongly modified the wettability by strengthening its hydrophobic state especially for the probing liquids with large polar components of the surface free energy [ethylene glycol, formamide, water (Table 1)]. For instance, the water contact angle increased from 3° after UV illumination to 85° after electron treatment.

Zisman plots (Fig. 3a, b) were constructed by plotting the found cosine of the measured contact angles on the diamond and ZnO powders versus surface tension of the tested liquids (Table 1). Zisman plot is linear (γ_{LV}). In all plots, a linear regression line was fitted, and the value of surface tension at $\cos\theta = 1$ (i.e., $\theta = 0$) was calculated from the resulting regression equation, which corresponds to the value of critical surface tension. The diamond powder (Fig. 3a) shows relatively low critical surface tension for untreated diamond particles (around 27 mJ/m^2), which is consistent with the observed moderate hydrophobicity. The low-energy electron irradiation leads to decrease in its critical surface tension to 23 mJ/m^2, while UV illumination increases it to 32 mJ/m^2.

Identical tendency was found for ZnO nanomaterial (Fig. 3b). The data show that the critical surface tension for untreated ZnO powder is approximately 37 versus 27 mJ/m^2 for diamond particles. The low-energy electron irradiation leads to the decrease in critical surface tension from 37 to 29 mJ/m^2. As a result of the UV treatment, it increases significantly to 70 mJ/m^2, providing high hydrophobic state of this nanomaterial. Thus, the range of the critical surface tension modification in ZnO is $\Delta = 41$ mJ/m^2, which exceeds the same parameter of the diamond particles by 4.5 times where $\Delta = 9$ mJ/m^2.

Figure 4 shows Owens–Wendt analysis plots, constructed in accordance with Eq. 4, for untreated, UV-illuminated and electron-irradiated diamond and ZnO powders.

The graphs show the expected linear Owens–Wendt relations (Fig. 4). The summarized results for diamond powder (Table 4) indicate that this nanomaterial possesses sufficient low surface energy $\gamma_{sv} = 33$ mJ/m^2, and it is consistent with the critical surface tension data (Fig. 3). The components of surface free energy $\gamma^p_{sv} = 8.5$ mJ/m^2 and $\gamma^d_{sv} = 24.5$ mJ/m^2, and fraction relation of the polar to the dispersive component is 0.35. The data show that the untreated diamond powder is characterized by moderate hydrophobic state, which is confirmed by the published data [37].

The calculated data (Table 4) illustrate that both surface modification UV treatments and electron beam weakly change the surface free energy and its components of diamond powder. The dispersive component γ^d_{sv} decreases feebly from 24.5 to 24 mJ/m^2 after UV treatment, the polar component grows from $\gamma^d_{lv} \sim 8.5$ mJ/m^2 to $\gamma^p_{sv} \sim 13$ mJ/m^2, leading the fraction relation to $\gamma^p_{sv}/\gamma^d_{sv} = 0.55$. Low-energy electron treatment of diamond particles is characterized by weak reduction in the surface energy and its components (mainly the polar component) of the irradiated material.

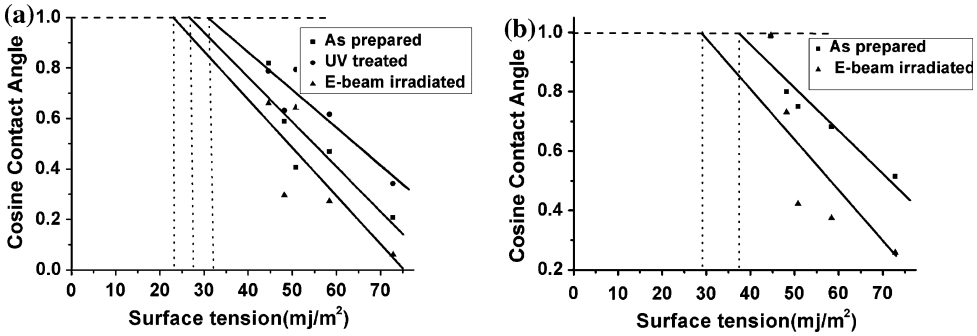

Fig. 3 Zisman plot of as-prepared (*squares*), UV-illuminated (*circles*), electron-irradiated (*triangles*) diamond (**a**) and ZnO (**b**) powders. The graph on UV treatment is not shown because of high wetting observed for all probing liquids. The statistical error was less than 2° for all investigated samples

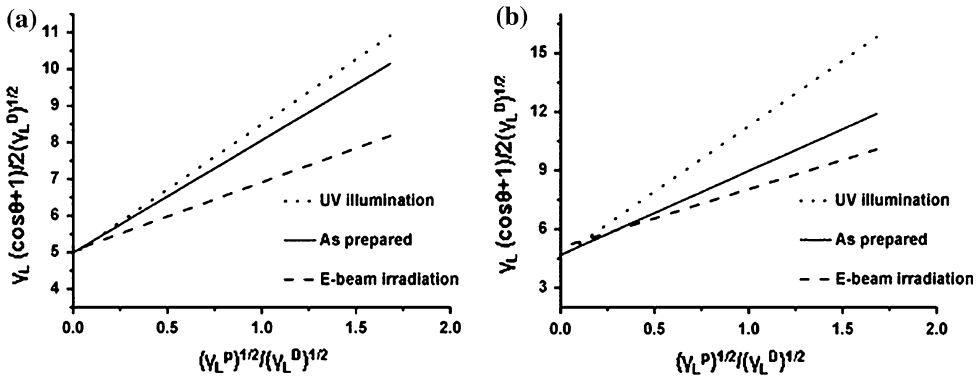

Fig. 4 Owens–Wendt analysis of as-prepared (*solid line*), UV-illuminated (*dot line*) and electron-irradiated (*dash line*) diamond (**a**) and ZnO (**b**) powders (the experiments were implemented with 6 different probing liquids presented in Table 1)

Table 4 Diamond nanoparticle surface free energy and its dispersive (γ_{sv}^{d}) and polar (γ_{sv}^{p}) components (in mJ/m^2) (Owens–Wendt analysis) for untreated and modified surfaces

	Polar component γ_{sv}^{p} (mJ/m^2)	Dispersive component γ_{sv}^{d}(mJ/m^2)	Surface energy γ_{sv}(mJ/m^2)	Fraction relation of the polar to the dispersive component
Untreated	8.5	24.5	33	0.35
UV illuminated	13	24	37	0.55
E-beam irradiated	3.5	25	28.5	0.15

The standard deviation of surface free energy and its components values does not exceed 2%

Table 5 ZnO powder surface free energy and its dispersive (γ_{sv}^{d}) and polar (γ_{sv}^{p}) components (in mJ/m^2) (Owens–Wendt analysis) for untreated and modified surfaces

	Polar component γ_{sv}^{p} (mJ/m^2)	Dispersive component γ_{sv}^{d}(mJ/m^2)	Surface energy γ_{sv} (mJ/m^2)	Fraction relation of the polar to the dispersive component
Untreated	18.5	22	40.5	0.8
UV illuminated	45	21	66	2.1
E-beam irradiated	9	25	34	0.35

The standard deviations of surface free energy and its components values do not exceed 2%

The summarized results for ZnO nanomaterial (Table 5) show that as-prepared ZnO nanomaterial possesses higher surface free energy $\gamma_{sv} = 40.5$ mJ/m^2 than that of diamond $\gamma_{sv} = 33$ mJ/m^2, which is provided by larger contribution of the polar component. The dispersive components are almost equal for these two materials. For ZnO, the fraction relation of the polar to the dispersive component reaches the value 0.8 compared with 0.35 for diamond. Untreated ZnO nanomaterial is slightly hydrophilic and has higher level of wettability compared to diamond, which is clearly defined by higher polar component of the surface free energy.

ZnO demonstrates high affinity to the surface modification. UV illumination leads to increasing surface free energy value γ_{sv} from 40.5 to 66 mJ/m^2. The found variations are mainly provided by the contribution of the polar component. It strongly grows from $\gamma_{sv}^{p} \sim 18.5$ mJ/m^2 to $\gamma_{sv}^{p} \sim 45$ mJ/m^2, leading the fraction relation to $\gamma_{sv}^{p}/\gamma_{sv}^{d} = 2.1$. Such a growth found for the modified diamond powder was much weaker with $\gamma_{sv}^{p}/\gamma_{sv}^{d} = 0.55$. These data are consistent with the critical surface tension measurements (Fig. 3). As a result of UV illumination of ZnO nanomaterial surface, high hydrophilic behavior was observed (Fig. 2a). Low-energy electron treatment was characterized by the opposite effect. Decrease in the surface free energy to 34 mJ/m^2 was found, which occurs due to decrease in the polar component γ_{sv}^{p} twice from ~ 18.5 mJ/m^2 to $\gamma_{sv}^{p} \sim 9$ mJ/m^2, while the dispersive component increased slightly up to 25 mJ/m^2. The fraction relation $\gamma_{sv}^{p}/\gamma_{sv}^{d}$ falls down to 0.35. Combination of these two modification methods varied the surface free energy in a wide range of 34–66 mJ/m^2.

Thus, for both studied powders, surface free energy and wettability modification occurred due to variation of the polar components. This conclusion was also confirmed by our calculations using van Oss-Chaudhury-Good approach [34], which showed dramatic variation of electron-acceptor component related to a polar sort of surface interactions.

Electron- and UV-Induced Surface Modification of Powders

The experiments conducted and the implemented estimations allow finding basic features of surface modification of two powders of different origins, diamond and ZnO. UV illumination leads to increasing the surface free energy making the surface hydrophilic, while the electron treatment generates an opposite effect and induces hydrophobicity. The found modifications are highly pronounced for ZnO nanomaterial and look much weaker for diamond particles. Both methods vary the polar component of surface free energy. UV treatment increases this component, but the electron irradiation decreases it.

The observed variation of the polar component is a direct evidence of deep modification of elementary physical interactions with the studied surfaces. Polar interactions include a few basic purely electrostatic interactions that involve the charge of ions and the permanent dipole of polar molecules. Charge–charge, charge–dipole and dipole–dipole interactions (Debye interactions) belong to this category as well as orientation interactions (Keesom interactions). UV treatment of diamond particles, strengthening the polar component, decreases slightly the

dispersive component. UV light causes decomposition of organic contaminations on solid surfaces and leads to surface cleaning [38, 39]. It stimulates adsorption of atmospheric water on the diamond surface [40]. Such a modification leads to increasing its hydrophilic state.

Our experimental data show that UV illumination influences much stronger ZnO nanomaterial occurring due to the enhancement of the polar component. ZnO possesses wurtzite hexagonal structure affording spontaneous electrical polarization and consequently piezoelectricity and pyroelectricity. Its UV-induced strong hydrophilicity may be ascribed to two different factors increasing polar forces: electrostatic interaction of a pyroelectric origin and its photosensitivity. High-energy photons supplied by UV source generate electron–hole pairs in ZnO nanomaterial that leads to the formation of surface oxygen vacancies and Zn^{+} defective sites [25]. The water and oxygen molecules may coordinate on the photogenerated surface defective site, which leads to dissociative adsorption of the water molecules on the surface. The defective sites on ZnO surface are kinetically more favorable for hydroxyl adsorption than for oxygen adsorption [36], and as a result, the surface hydrophilicity is dramatically improved and the water contact angle on ZnO nanomaterial surface changes from 60° to 3°. It should be noted that the same considered polar forces of various origins provide extremely high affinity of ZnO nanoparticles to self-assembling into ordered nanostructures [24] due to the enhancement of cohesive interactions followed by agglomeration (Fig. 1a). It should be marked that the UV variation of hydrophilicity is much weaker in diamond particles as well as its affinity to agglomerate where diamond intrinsic inertness is unique and cannot be sufficiently modified.

The observed growth of hydrophobicity in both sorts of powders under low-energy electron irradiation and the observed decreasing of polar component may be explained by electron-induced formation of carbon-rich layer on the surface. This phenomenon has been observed by us in more than 20 solid-state materials of different origins [13, 21]. In the work of Hillier [41], it has been shown that the carbon contamination deposited under electron beam irradiation is formed by the reaction of the incident electrons with organic molecules on the irradiated surface. The electron-deposited organic CH_2-layer [20, 21] possesses major dispersive component and leads to a strong hydrophobicity.

Pronounced effect of electron-induced surface modification was found for macroscopic wettability behavior of ZnO nanomaterials (Fig. 2). High hydrophilic state induced by UV illumination was converted to extremely high hydrophobic state due to low-energy electron irradiation. It should be noted that the wettability effect is very sensitive to surface defects [42, 43], which might be generated by the electron beam. The applied electron irradiation energy in our experiments was $E_p = 300$ eV. The chosen electron energy is less by 3 orders of magnitude than the threshold energy for atomic displacement in ZnO and generation of point defects in its lattice [44]. So far, unusually high hydrophobicity observed on ZnO nanomaterial was generated due to the modification of elementary interface interaction forces. Obviously, such a strong water repellency induced by electron irradiation is amplified by highly developed surface area of the nanomaterial.

Conclusions

We have conducted studies of surface modification and basic interface interactions in two powders of different origins, diamond and ZnO. The developed surface modification technique based on combination of low-energy electron irradiation and UV illumination has resulted in surface free energy and wettability modification in a wide range of water contact angles. It has been shown that UV illumination turns the ZnO nanomaterial surface to high hydrophilic state, while a low-energy electron irradiation leads to water repellency. Much weaker wettability modification was observed in diamond particles. The found difference is related to inherent different physicochemical natures of ZnO and diamond powders.

Detailed thermodynamic studies using different classical approaches have allowed us to show that UV and electron beam irradiation strongly modify the surface free energy due a deep modulation of its polar component, resulting in variation of elementary surface interactions.

The electron-induced modification of the surface free energy is a completely new concept for nanomaterials, and the present work proposes an effective technological approach for controlling variation of their key surface-related properties such as wettability, cohesion and agglomeration.

Acknowledgment This work was supported by the Israel Science Foundation, grant number 960/05.

References

1. D.K. Pritchard (2004), HSL Report EC/04/03. Published on HSE website
2. M. Lazghab, K. Saleh, I. Pezron, P. Guigon, L. Komunjer, Powder Technol. **157**, 79 (2005)
3. G. Nichols, S. Byard, M.J. Bloxham, J. Botterill, N.J. Dawson, A. Dennis, V. Diart, N.C. North, J.D. Sherwood, J. Pharm. Sci. **91**, 2103 (2002)
4. K. Uematsu, H. Morohashi, T. Morimoto, N. Uchida, K. Saito, J. Mater. Sci. Lett. **8**, 1011 (1989)
5. S.H. Jung, S.H. Park, D.H. Lee, S.D. Kim, Polym.Bull. **47**, 199 (2001)
6. A. Kudrolli, Nat. Mater. **7**, 174 (2008)

7. Y. Min, M. Akbulut, K. Kristiansen, Y. Golan, J. Israelachvili, Nat. Mater. **7**, 527 (2008)
8. C. Bayer, M. Karches, A. Matthews, P.R. von Rohr, Chem. Eng. Technol. **21**(5), 427 (1998)
9. W. Gang, M. Yuedong, Z. Shaofeng, L. Feng, J. Zhongqing, S. Xingsheng, R. Zhaoxing, W. Xiangke, Plasma Sci. Technol. **10**(1), 78 (2008)
10. D. Vollath, D.V. Szab'o, J. Nanopart. Res. **1**, 235 (1999)
11. B. Pukánszky, E. Fekete, Adv. Polym. Sci. **139**, 1436 (1999)
12. P.K. Chu, J.Y. Chen, L.P. Wang, N. Huang, Mater. Sci. Eng: R: Reports. **36**(5–6), 143 (2002)
13. G. Rosenman, D. Aronov, Yu. Dekhtyar, Wettability Engineering in Solid State Materials. PCT Patent, WO 2007/049380 A1, 2007
14. D. Aronov, M. Molotskii, G. Rosenman, Appl. Phys. Lett. **90**, 104104 (2007)
15. I. Torchinsky, G. Rosenman, Appl. Phys. Lett. **92**, 052903 (2008)
16. V. Sabaev, D. Aronov, G. Rosenman, Appl. Phys. Lett. **93**, 1444104 (2008)
17. D. Aronov, R. Rosen, E.Z. Ron, G. Rosenman, Process Biochem. **41**, 2367 (2006)
18. D. Aronov, R. Rosen, E.Z. Ron, G. Rosenman, Surf. Coat. Technol. **202**, 10–2093 (2008)
19. D. Quere, Rep. Prog. Phys. **68**, 2495 (2005)
20. D. Aronov, G. Rosenman, Surf. Sci. **601**, 5042 (2007)
21. D. Aronov, M. Molotskii, G. Rosenman, Phys. Rev. B. **76**, 035437 (2007)
22. K. Larsson, H. Björkman, K. Hjort, J. Appl. Phys. **90**(2), 15 (2001)
23. A. Krueger, Adv. Mater. **20**, 2445 (2008)
24. Z.L. Wang, J. Phys, Condens. Matter. **16**, R829 (2004)
25. R.-D. Sun, A. Nakajima, A. Fujishima, T. Watanabe, K. Hashimoto, J. Phys. Chem. B **105**, 1984 (2001)
26. A. Siebold, A. Walliser, M. Nardin, J. Colloid. Interface Sci **186**(1), 60 (1997)
27. C.A. Prestidge, G. Tsatouhas, Int. J. Pharm. **198**(2), 201 (2000)
28. Zs Tüskea, G. Regdon Jr, I. Erősa, S. Srčičb, K. Pintye-Hódi, Powder Technol. **155**(2), 169 (2005)
29. E.W. Washburn, Phys. Rev. **17**, 273 (1921)
30. P. Luner, E. Oh, Colloids surf A. Physicochem Eng Asp. **181**, 31 (2001)
31. S. Siboni, C. Della Volpe, D. Maniglio, M. Brugnara, J. Colloid. Interface Sci. **271**, 454 (2004)
32. H.W. Fox, A.W. Zisman, J. Colloid. Sci. **6**, 514 (1950)
33. D.K. Owens, R.C. Wendt, J. Appl. Polym. Sci. **13**, 1741 (1969)
34. C.J. Van Oss, R.J. Good, M.K. Chaudhury, Langmuir. **4**, 884 (1988)
35. W. Jańczuk, W. Wójcik, A. Zdziennicka, J. Colloid. Interface Sci. **157**, 384 (1993)
36. X. Feng, L. Feng, M. Jin, J. Zhai, L. Jiang, D. Zhu, J. Am. Chem. Soc. **126**, 62–63 (2004)
37. F. Pinzari, P. Ascarellia, E. Cappellia, G. Matteia, R. Giorgib, Diam Relat Mater. **10**, 781 (2001)
38. J.R. Vig, J. Vac. Sci. Technol. A. **3**, 1027 (1985)
39. D.W. Moon, A. Kurokawa, S. Ichimura, H.W. Lee, I.C. Jeon, J. Vac. Sci. Technol. A. **17**, 150 (1999)
40. L.M. Apatiga, R. Velazques, V.M. Castano, Surf. Sci. **529**, 158 (2003)
41. J.J. Hiller, J. Appl. Phys. **19**, 226 (1947)
42. V.A. Bakaev, W.A. Steele, J. Chem. Phys. **111**, 9803 (1999)
43. E.A. Leed, J.O. Sofo, C.G. Pantano, Phys. Rev. B. **72**, 155427 (2005)
44. T. Yoshiie, H. Iwanaga, N. Shibata, M. Ichihara, S. Takeuchi, Philos. Mag. **A40**(2), 297 (1979)